Eur. Phys. J. D **4**, 131–137 (1998)

THE EUROPEAN PHYSICAL JOURNAL D

© EDP Sciences
Springer-Verlag 1998

Photo induced collisions with laser cooled He* atoms

H.C. Mastwijk, M. van Rijnbach, J.W. Thomsen, P. van der Straten[a], and A. Niehaus

The Debye Institute, University of Utrecht, P.O. Box 80.000, 3508 TA Utrecht, The Netherlands

Received: 9 February 1998 / Revised: 4 May 1998 / Accepted: 14 May 1998

Abstract. This paper presents an experimental investigation of cold collisions between metastable helium atoms in an optical trap at 1 mK. Penning (PI) and associative (AI) ionization reactions are distinguished using a mass spectrometer and studied under influence of near resonant laser light. Dramatic enhancement, by more than a factor 15, of the ion rate is observed when the laser is tuned close to resonance. Experimental findings are well-described, on an absolute scale, by model predictions.

PACS. 32.80.Pj Optical cooling of atoms; trapping – 33.80.Eh Autoionization, photoionization, and photodetachment – 34.50.Rk Laser-modified scattering and reactions

1 Introduction

The ability to trap and manipulate neutral atoms by means of laser light have created new fascinating environments for studies of atomic interactions at low temperatures [1,2]. With the invention of the magneto-optical trap (MOT), dense and cold samples of atoms are now produced routinely and studied under controlled conditions. Collision dynamics of cold atoms have recently attracted considerable attention experimentally as well as theoretically [3–9]. When a near resonant light field is introduced into the cold atom cloud the rate coefficient for collisional processes can be dramatically modified [9]. As two slowly moving atoms approach they form a quasi molecule which can be excited during the collision. If the molecular complex is excited to a repulsive energy state the atoms will be pushed apart thus preventing them from reaching small internuclear distances where reactions may take place. This effect is called optical shielding of collisions and has been observed in several systems [6,10]. In the case of a light field detuned below the atomic resonance, excitation to an attractive potential curve will take place. Note, that the interaction potential will depend critically on the electronic state of the atoms involved. When the two atoms are in the ground state we have a van der Waals interaction which scales as $1/R^6$. With one atom in an excited P-state, the potential energy arises from an induced dipole-dipole interaction scaling as $1/R^3$. Since the excited state potential reduces the centrifugal barrier more partial waves will contribute in the collision process, exemplified for the He*–He* system in Figure 1. Typically only zero or one partial wave come in play for colliding atoms in the ground state at mK temperatures while usually 5–10 partial waves will contribute for the excited state potential.

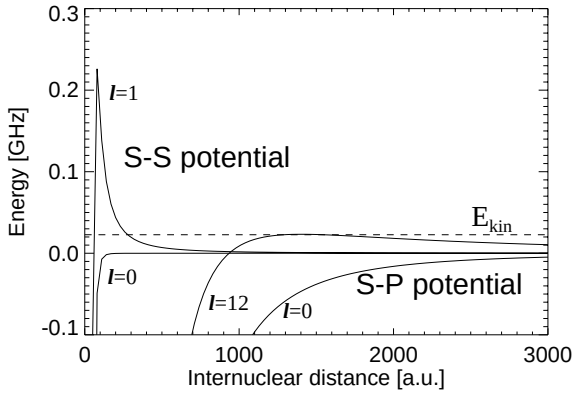

Fig. 1. Lowering of the centrifugal barrier in the excited state for the He*–He* system. The ground state $S-S$ potential scales as $1/R^6$ and has a centrifugal barrier, which is already for $\ell = 1$ too high to overcome. The excited state $S-P$ potential scales as $1/R^3$, which for a temperature of 1 mK allows 12 partial waves to reach short internuclear distances.

Interaction with the light field, leading to excitation, spontaneous emission and stimulated emission of the quasi molecule, is an intrinsic part of the cold collision dynamics and offers additional room for influencing the outcome of a collision event. Here the lifetime of the atom in question is important as well as the power and polarization of the light used to probe the collision. This situation is in sharp contrast to collisions with laser prepared atoms at thermal or higher temperatures. Here light is used to excite an independent, isolated atom which then collides with another particle.

The present experiment addresses optical collisions between cold metastable triplet atoms in an optical trap at 1 mK. The atoms may be in the He(2^3S) ground state

[a] e-mail: P.vanderStraten@fys.ruu.nl

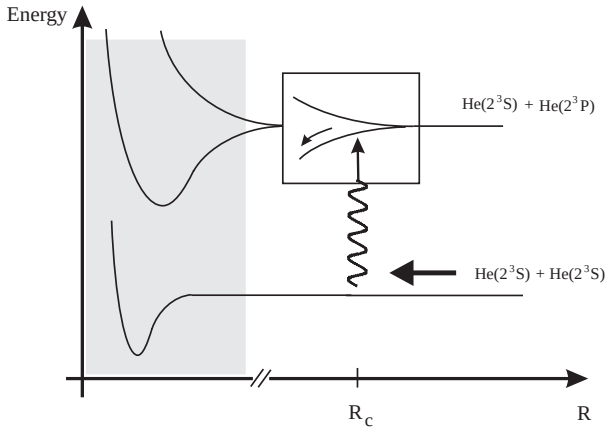

Fig. 2. The quasi molecule formed by two metastable atoms in the $S-S$ ground state is excited to the $S-P$ state at the Condon point R_c, where the laser frequency equals the dipole-dipole interactions energy. If the laser detuning is negative, as shown in figure, the molecular $S-P$ complex is accelerated towards small internuclear distances where ionization reactions may take place, indicated by the shaded box.

or the $\mathrm{He}(2^3P)$ excited state and will spontaneously Penning ionize if their internuclear distance becomes sufficiently small

$$\mathrm{He}(2^3S) + \mathrm{He}(2^3S, 2^3P) \rightarrow \begin{cases} \mathrm{He}^+ + \mathrm{He}(1^1S) + e^- \\ \mathrm{He}_2^+ + e^- \end{cases} . \quad (1)$$

Depending on the energy transferred to the electron the ion products may end up as an atomic ion (He^+) or a molecular ion (He_2^+). Monitoring this ion yield as a function of the light field frequency provides detailed information on the long-range interaction between two slowly colliding metastable atoms. This is illustrated in Figure 2.

A red detuned photon transfers the He*–He* complex to the attractive part of the excited state potential at the Condon point R_c. Here it is accelerated towards small internuclear distances where ionization may occur. Inevitably spontaneous decay of the $S-P$ complex will reduce the chance of reaching small distances on the excited state potential. Depending on the absolute value of the detuning, *i.e.*, the location of R_c, the chance of decaying varies. This can be controlled by adjusting the frequency of the photons.

The He* collision system possesses several attractive features compared to other systems investigated so far. Having no nuclear spin the He atoms do not suffer from the presence of hyperfine structure. This facilitates considerably interpretation of data and offers the possibility of accurate and detailed modeling on an absolute scale.

Yet another property of the He* system is interesting. Two distances characterize an optical collisions: $R_\tau = v\tau$, the average distance traveled by an atom during one lifetime, and $R_\lambda = \lambda/2\pi$, the characteristic length where retardation effects become important. Although R_λ is in the same order of magnitude for all systems studied so far, R_τ is two orders of magnitude larger for the He*+He* system compared to the other systems, as seen from Table 1. Therefore we expect the He* system to be different from other systems and, in addition, retardation effects to become important.

Table 1. Critical distances R_τ of molecular excitation that have been accessed in optical collision experiments. Reactions are studied for molecular excitations in the He*+He* system far beyond the point of R_λ.

system	λ [nm]	τ [ns]	$\langle v \rangle$ [m/s]	R_τ [Å]	R_λ [Å]	Ref.
He*+He*	1083	98	2.0	2744	1724	[14]
Na+Na	589	16	0.3	65	940	[3,7,8]
Kr*+Kr*	811	31	0.2	87	1290	[5]
Rb+Rb	780	27	0.1	45	1240	[4]
Xe*+Xe*	882	33	0.1	42	1404	[6]

2 Experimental setup

The experimental setup consists of three main sections separated by differential pumping stages; a metastable helium source, a Zeeman slower, and a magneto-optical trap, shown schematically in Figure 3. Metastable atoms are produced in a high pressure DC discharge expanding through a small 0.5 mm nozzle hole. To reduce the initial atom velocity the source unit is cooled with liquid nitrogen and operated at a low discharge power (700 V, 3 mA). Under these conditions we have a $\mathrm{He}(2^3S_1)$ output yield of 10^{14} $\mathrm{sr}^{-1}\mathrm{s}^{-1}$ with a mean beam velocity of 900 m/s. Before the metastable atoms can be loaded into the MOT they must be slowed down sufficiently. In the Zeeman slower the atoms are decelerated by a counter propagating laser beam tuned close to the $\mathrm{He}(2^3S_1)$–$\mathrm{He}(2^3P_2)$ transition. A spatial varying magnetic field along the beam axis provides a Zeeman detuning which keeps the atoms in resonance through the slower unit. By optimizing the current in the Zeeman coils, and the laser detuning, final velocities in the range of 50−100 m/s can be obtained. Even lower velocities are attainable but at the expense of a significant transverse expansion of the beam. Ultimately the beam will fan out and this results in a poor beam intensity at the trap position. In the MOT section the atoms are further decelerated and finally trapped. The MOT is composed of three pairs of counter propagating laser beams crossing at right angles in the center of a quadrupole magnetic field. The quadrupole field is generated by two circular coils mounted in an anti-Helmholtz configuration. Typical field gradients are 7.5 G/cm in the plane of the coils and 15 G/cm along the center axis perpendicular to the coil plane.

A detailed picture of the optical setup is given in Figure 4. Both slowing and trapping lasers are operated on the $\mathrm{He}(2^3S_1)$–$\mathrm{He}(2^3P_2)$ transition of metastable helium. The 1083 nm laser light required for this transition is provided by two SDL single mode diode lasers, each capable of giving an output power of 50 mW. For trapping, we use a single laser beam. Two telescopes optimize circular

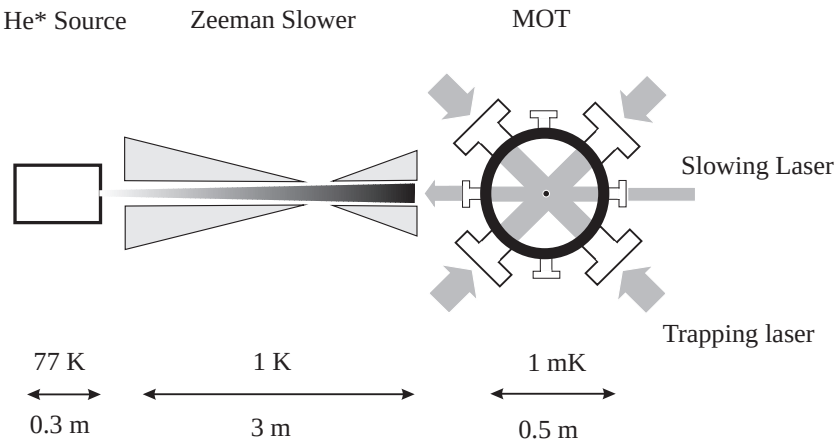

Fig. 3. Schematic view of the experimental setup from above. A beam of metastable atoms is produced in a DC discharge. After being decelerated in a Zeeman slower by a counter propagating laser beam the atoms are loaded into a magneto-optical trap. Here the atoms are further cooled and studied.

beam shape and diameter while a Glan-Thomson polarizer, followed by a $\lambda/4$-plate, ensures the right circular polarization state of the light before it enters the trap region. First the trap beam traverses the symmetry plane of the MOT coils, then mirrored out of the plane and directed along the center axis of the coils, and finally reflected back by a mirror placed under the MOT chamber (not shown). A $\lambda/2$-plate changes the helicity of the laser light just before it is mirrored out of the symmetry plane while a $\lambda/4$-plate on top of the back reflecting mirror ensures correct polarization state for the back going light beam.

To acquire an optimal loading rate of the MOT it is operated at a large negative detuning of 15Γ (natural line width $\Gamma = 1.6$ MHz), a high trap laser power of 50 I_0 (saturation intensity $I_0 = 0.16$ mW/cm^2), and with a large trap beam diameter of about 35 mm (full width at $1/e^2$-height). The latter increases the capture velocity and capture area of the MOT. With a background pressure of 3×10^{-9} mbar we typically trap about 10^5 atoms in a volume of 1 mm^3 yielding an average density of about 10^8 atoms/cm^3. The lifetime is typically 3–4 s.

For diagnostics of the trapped atom cloud we have installed a mass spectrometer and a micro channel plate, both mounted in the symmetry plane of the two circular coils but opposite to each other, as shown in Figure 4. A plate mounted in front of the mass spectrometer is biased by a small negative voltage (typical -150 V) in order to extract ions originating from the MOT volume. The ions may be formed in collisions between slow helium atoms in the MOT (see Eq. (1)) or in Penning ionization with background gas atoms. In particular, mass selective detection allows a discrimination between Penning and associative ionization reactions, taking place between the cold atoms, as well as ionization with "hot" background particles. A grid mounted in front of the microchannel plate (MCP) can be biased negative (typical -400 V) when the total ion yield is measured, or positive (typical $+100$ V) when only metastable atoms are detected. When the MOT is operating, we observe a total ion yield of about 25 kHz mainly due to Penning ionization with the background gas.

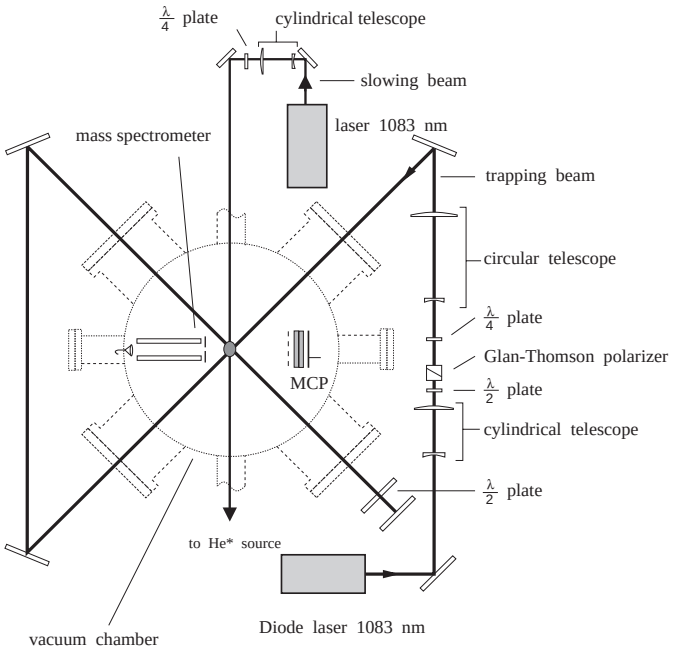

Fig. 4. Detailed picture of the optical setup used for trapping and slowing. Two diode laser systems are used, one for initial slowing of the atoms and the second for trapping of the atoms. A mass spectrometer and a microchannel plate is mounted close to the MOT center for diagnostics of the cold atoms.

The temperature of the atom cloud was measured by a time of flight technique. Biasing the MCP grid by a positive voltage and releasing the atom cloud to expand freely in the gravitational field we could measure the flight time to the MCP located 70 mm from the MOT center. Figure 5 shows the result of such a measurement. The time of flight distribution is peaked at about 30 ms corresponding to an average velocity of about 2 m/s. By fitting a Maxwell-Boltzmann distribution to the measured data we

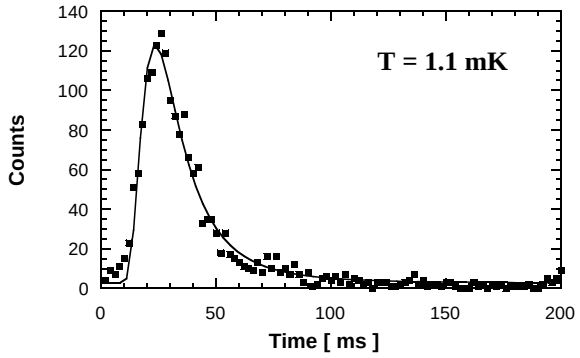

Fig. 5. Time of flight distribution of cold metastable atoms after being released from the MOT. The temperature is found to be about 1mK which corresponds to a mean velocity of 2 m/s.

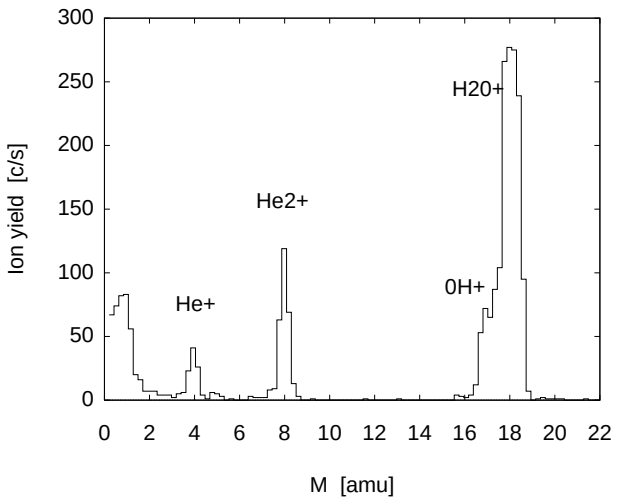

Fig. 6. Ion mass spectra from the MOT. The He^+ and He_2^+ peaks are produced in collisions between cold metastable atoms in the MOT. The H_2O^+ is produced in Penning ionization with water molecules on trapped He* atoms.

obtain a temperature of 1.1 mK in good agreement with prediction of standard Doppler theory using our MOT parameters [11]. In addition, we obtain an estimate for the total number of atoms in the MOT. Knowing the exact area of the MCP we can correct for the solid angle and obtain about 10^5 atoms, consistent with the total ion rate measurement.

3 Results and discussion

This section presents results on optical collision experiments with cold metastable triplet atoms at 1 mK. Collisions between the slow atoms in the trap and background atoms produces an ion rate

$$R = \alpha N + \frac{\beta}{2} \int n(\boldsymbol{r})^2 d\boldsymbol{r} \tag{2}$$

where $N = \int n(\boldsymbol{r}) d\boldsymbol{r}$ is the total number of atoms in the trap, α is characterizing the production of ions in collisions with background gas atoms and β the PI and AI rate as defined in equation (1). The α coefficient is related to the cross-section by

$$\alpha = \sum_i \sigma_i n_{bg}^i \bar{v}_i \tag{3}$$

with σ_i being the ionization cross-section of metastable helium colliding with the background atoms of type i, n_{bg}^i the density and $\bar{v}_i$ the average velocity of the background atoms. For the β coefficient we have

$$\beta = \sigma_* \bar{v}_r \tag{4}$$

where the σ_* is the cross-section for PI and AI ionization and $\bar{v}_r$ the average relative velocity between metastable atoms in the MOT. The density profile of the MOT is given by $n(\boldsymbol{r})$ and is well-approximated by a Gaussian distribution function.

Figure 6 shows results of a mass spectrum taken when the trap was in operation. Two remarkable features are observed. Firstly, two clear peaks appear at mass 4 amu and 8 amu which we identify with the formation of He^+ and He_2^+ ions produced in collisions between trapped helium atoms. They cannot be produced in collisions with the background gas or the loading beam, since the density is several orders lower compared to the MOT density. The two peaks have different height indicating different reaction rates of the PI and AI process defined in equation (1). Unfortunately the ions are not detected with the same efficiencies. The He_2^+ ion is produced with a very low velocity and is detected with a high efficiency. The He^+ ion is produced with a significant higher velocity due to the dissociation of the molecular ion. This reduces the extraction efficiency of the He^+ ions. In order to correct for this we simulated the extraction of the ions by calculating the trajectories for different initial velocities, obtained using the potential in [12]. This gave correction factors for the measured ion yield. Secondly, the large peak at 18 amu is associated with Penning ionization with water on cold He* atoms. This peak is due to a cross-section of this process of more than 70 $\mathring{A}^2$ [13]. Using the mass spectrometer we are able to distinguish collisions taking place in the MOT, between slow metastable atoms, and collisions with the background atoms. In the following we will concentrate on intra MOT collisions, *i.e.*, the peaks with mass 4 amu and 8 amu.

In the mass spectrum shown above we have a mixture of atoms with about 80% in the ground state (2^3S_1) and 20% in the excited state (2^3P_2). It is desirable to separate the signal contributions arising from collisions between atoms in the ground state and the excited state. Figure 7 presents results from an experiment in which we detected He_2^+ ions. The MOT laser is detuned far below resonance in a short time interval and then returned to normal trapping operation. The time interval is chosen to be of the order of 20 μs, which is long compared to the natural lifetime of 100 ns but short compared to the expansion time of the

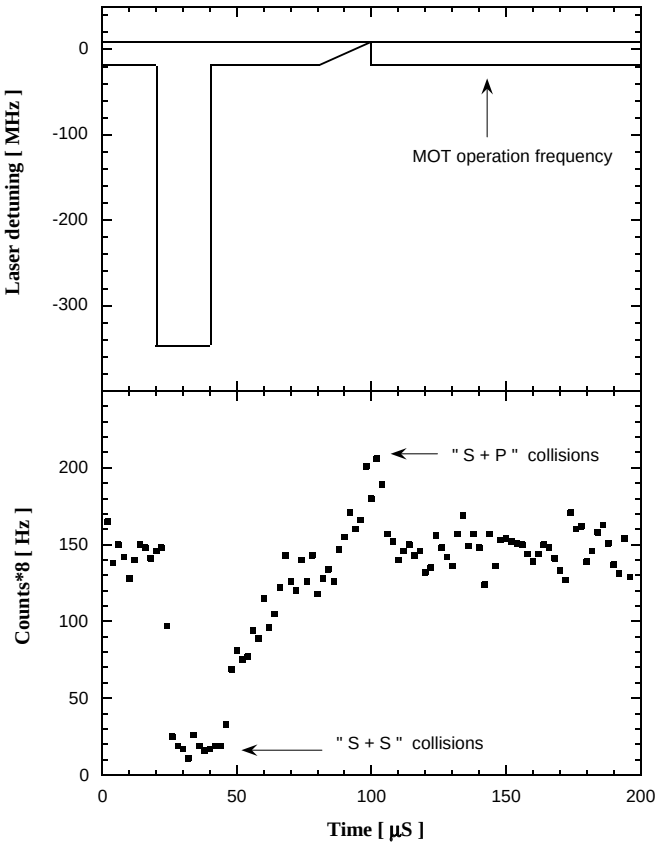

Fig. 7. Optical modulation of the He_2^+ ion yield. The laser is first detuned far below resonance, then ramped to resonance and finally returned to the normal trapping frequency. Notice the dramatic effect when the laser is shifted off resonance and only atoms in the ground state is present. Close to the $He(2^3S_1)$–$He(2^3P_2)$ resonance a fraction of the cold atoms are in the excited state enhancing the ion production significantly.

atom cloud. The scan cycle is repeatedly integrated until satisfactory statistics is obtained. We observe a dramatic drop in the He_2^+ ion production as the laser is shifted off resonance. Since the laser is detuned about 350 MHz below the atomic transition frequency only ground state $He(2^3S)$ atoms are present. The ion production thus takes place *via* interaction on the potentials $1^1\Sigma_g^+$, $1^3\Sigma_u^+$ and $1^5\Sigma_g^+$, connecting asymptotically to $He(2^3S)$–$He(2^3S)$ manifold. The quintet state, however, will not contribute due to violation of the total spin conservation in the ionization process. When the laser is shifted to resonance the ion yield increases strongly. Now the MOT contains, in addition to atoms in ground state a fraction of atoms in the excited 2^3P_2 state. Considering the high powers used for the trapping laser we assume the number of excited atoms to be 50% on resonance. The significant enhancement of the ion yield at resonance we ascribe to an increased ion rate when atoms react *via* the excited state $He(2^3S)$–$He(2^3P_2)$ potential. The reason is twofold. Firstly, the attractive nature of the $S-P$ dipole-dipole interaction "captures" more partial waves compared to the $S-S$ potential (see Fig. 1).

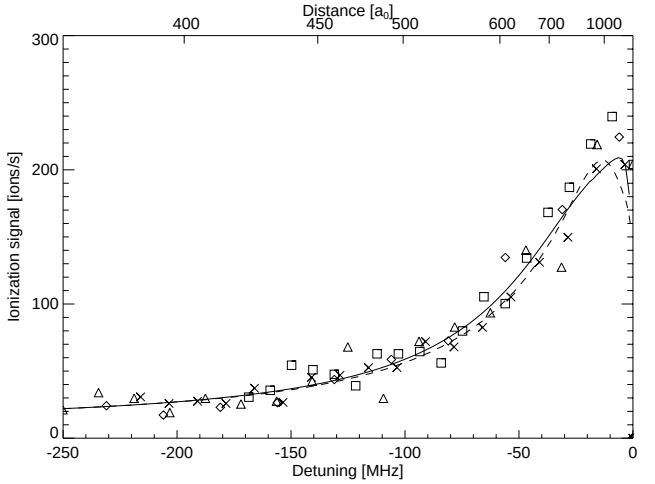

Fig. 8. The frequency dependence of the He_2^+ ion yield. The solid line represents the our semi-classical model calculation and the dashed lined is predictions of a modified JV-model. Both are in very good agreement with the absolute rate measured.

The number of contributing partial waves for the $S-P$ potential is about 10 while only the $l = 0$ wave contributes for the $S-S$ potential at 1 mK. Secondly, the lifetime of the $S-P$ complex is very long so once excited, even at large internuclear distances, it will survive until it reaches small distances where ionization occurs. This is in contrast to all other systems investigated. The characteristic distance, R_τ, traveled for these systems is, as seen from Table 1, more than one order of magnitude less compared to the He* system. As the laser frequency is tuned close to resonance the ion rate drops rapidly for these systems since the excited quasi molecules do not live long enough to reach small internuclear distances.

We have measured the ratio of He_2^+/He^+ on and off resonance. Corrected for the transmission efficiency we find, on resonance 0.16 ± 0.02 and off resonance 0.03 ± 0.003, where the error bars refer to statistical uncertainties. Using our known MOT parameters for the number of atoms and the trap volume we deduce the rate coefficient for $S-S$ collisions to be $(2.7 \pm 1.2) \times 10^{-10}$ cm^3/s and for $S-P$ collisions $(1.9 \pm 0.8) \times 10^{-9}$ cm^3/s. The $S-P$ rate is noted to be a factor of 100 less than previous values reported for this system [14]. Based on the ground state $He(2^3S)$–$He(2^3S)$ potentials [12] quantum mechanical calculations of the $S-S$ rate coefficient have been carried out, yielding 7.3×10^{-11} cm^3/s in very good agreement with the measured rate [15].

To explore further the dynamics of the collision at long internuclear distances we measured the He_2^+ ion yield as a function of the trap laser frequency. In a time interval of about 50 μs the trap laser is linearly shifted to -300 MHz while the He_2^+ ion signal is monitored. Figure 8 shows results of several such measurements. Near resonance the ion signal increases considerably and then drops gradually to the S–S rate as the laser detuning increases. At larger detunings, (≤ -50 MHz), the excitation of isolated

He* atoms is completely negligible but we still observe a relatively high ion rate. This is attributed to resonant excitation of transient molecules, *i.e.*, when two atoms approach to an internuclear distance close to the Condon point at which the laser frequency equals the dipole-dipole interaction energy.

4 Theoretical modeling

To describe the data as shown in Figure 8 we have developed a model based on semi-classical considerations. In this model we describe the excitation in the region of the Condon point $R_C = (C_3/\hbar\delta)^{1/3}$ within the dressed atom picture, in which a crossing between the potentials for ground and excited state of the quasi molecule arises. The flux of atoms crossing the Condon radius is given by the classical distribution function [16] $F = 4\pi R_c^2 n^2 v_{rad}$, with v_{rad} the radial velocity. The excitation probability at the Condon radius is calculated using the Landau-Zener expression [17]

$$P_{ex} = 1 - \exp(-\pi\Lambda), \tag{5}$$

with the Landau-Zener parameter Λ given by

$$\Lambda = \frac{2\hbar\Omega^2}{\alpha v}\,. \tag{6}$$

Here Ω is the Rabi-frequency and v the velocity of the atom. Furthermore, the parameter α is the slope of the interaction potential at the Condon point, which in this case is given by

$$\alpha = \left|\frac{dV}{dR}\right|_{R_c} = \frac{3C_3}{R_c^4}\,. \tag{7}$$

After excitation the two atoms are attracted towards each other due to the induced dipole-dipole interaction and they have a probability of Penning ionization at small internuclear distances. However, there are two constraints. Firstly, the quasi molecule has to reach small internuclear distances, where the ionization takes place. Secondly, the flight time may not be too large, since the lifetime of the quasi molecule in the excited state is in the same order as the atomic lifetime. Therefore the molecule can deexcite before reaching small internuclear distances by spontaneous emission.

In order to evaluate these constraints we have calculated classical trajectories for the quasi molecule. The trajectory of an atom, crossing the Condon radius with an initial velocity $\mathbf{v}$, is calculated and its "fate" is indicated with the parameter w. If the atom reaches small internuclear distances, we have $w = 1$, whereas we have $w = 0$, if not. From the calculation we extract the time interval τ_0 between the excitation at R_c and the arrival at small internuclear distance. The survival $S(\tau_0)$ of the atom in the excited state is described by an exponential decay $S(\tau_0) = \exp(-\Gamma\tau_0)$. If we combine all four steps (flux inwards, excitation, reaching close distances, in the excited state) we arrive at our final expression

$$R_{ion} = V\int_{-\pi/2}^{\pi/2} F(R_c)P_{ex}(R_c)w(R_c)S(\tau_0)\sin\theta\; d\theta/2, \tag{8}$$

where the integration over the angle θ runs over all angles of the initial velocity $\mathbf{v}$ with respect to the internuclear axis and V denotes the MOT volume.

Our model becomes identical to the model of Gallagher and Pritchard [16] in the case of low excitation rate and large detuning. However, we extend on it by including a Landau-Zener excitation probability instead of a quasi-static approximation, which does not produce correct results for high excitation rates. Furthermore, we explicitly calculate the trajectory of the atom, in order to determine, if under the initial conditions the atom can reach small internuclear distances. Our model becomes identical to the model proposed by Julienne and Vigue [18], when we replace their quasi-static excitation rate with the Landau-Zener expression. However, the model of Julienne and Vigue is based on a quantum-mechanical description of the dynamics, whereas we rely on a classical description.

The results of our calculations is shown in Figure 8 together with the measured data. The agreement between theory and experiment is satisfactory. In the calculation we have taken into account, that for the He*–He* system we have, due to the fine structure interaction, 10 attractive curves from which 9 can contribute to the ionization. For each of these curves we have carried out the calculation and finally performed the statistical weighted sum. Furthermore, we have averaged the calculation over the distribution of incoming velocities, which is determined by the temperature (1 mK) of the trap. There are some deviations at small detunings, but these are to be expected, since at small detunings the two dressed states come close together and the quasi molecule starts no longer from the lowest state. Then we expect that describing the excitation rate with the Landau-Zener expression becomes inaccurate. Also indicated in the figure by a dashed line the result of the Julienne-Vigue model, where we have replaced their quasi-static expression with the Landau-Zener expression. The agreement between the two models is excellent, indicating that both a classical and quantum-mechanical description of the dynamics work for our system.

5 Conclusion and outlook

We have studied collisions between slow metastable triplet He atoms in an optical trap. Characteristic for this system is its ability to ionize at short distances to atomic He^+ or molecular He_2^+ ions. Using a mass spectrometer we have been able to distinguish these two fundamental reaction channels. Significant enhancement of the ion rate is observed for both channels, when laser light is tuned close to the $He(2^3S_1)$–$He(2^3P_2)$ resonance. This increase takes place as a result of the relative long distance the helium atoms can travel in

the excited state. From detailed measurements we obtained a rate coefficient $(2.7 \pm 1.2) \times 10^{-10}$ cm^3/s for collisions between ground state atoms He(2^3S)–He(2^3S) and $(1.9 \pm 0.8) \times 10^{-9}$ cm^3/s for collisions between atoms in the ground state and excited state He(2^3S)–He(2^3P_2). Theoretical prediction of the $S-S$ rate coefficient, 7.3×10^{-11} cm^3/s, is in good agreement with the measured value. Experimental results involving the excited state are well-accounted for using a intuitive semi-classical description while ground state results requires full quantum treatment.

Future experiments will concentrate on optical shielding effects where the laser is tuned to the blue of the atomic resonance. Here the He* system takes a prominent place due to it simple level structure.

This work has been supported by the "Stichting voor Fundamenteel Onderzoek der Materie (FOM)", which is financially supported by the "Nederlandse organisatie voor Wetenschappelijk Onderzoek (NWO)" and JWT is supported by the European Union's TMR programme under contract number ERB4001GT95292.

References

1. H. Metcalf, P. van der Straten, Phys. Rep. **244**, 203 (1994).
2. P.D. Lett, P.S. Julienne, W.D. Phillips, Rev. Phys. Chem. **46**, 423 (1995).
3. P.D. Lett, K. Helmerson, W.D. Phillips, L.P. Ratliff, S.L. Ralston, M.E. Wagshul, Phys. Rev. Lett. **71**, 2200 (1993).
4. M.G. Peters, D. Hoffman, J.D. Tobiason, T. Walker, Phys. Rev. A **50**, R906 (1994).
5. H. Katori, F. Shimuzu, Phys. Rev. Lett. **73**, 2555 (1994).
6. M. Walhout, U. Sterr, C. Orzel, M. Hoogerland, S.L. Rolston, Phys. Rev. Lett. **74**, 506 (1995).
7. P.A. Molenaar, P. van der Straten, H.G.M. Heideman, Phys. Rev. Lett. **77**, 1460 (1996),
8. J.J. Blangé, J.M. Zijlstra, A. Amelink, X. Urbain, H. Rudolph, P. van der Straten, H.C.W. Beijerinck, H.G.M. Heideman, Phys. Rev. Lett. **78**, 3089 (1997).
9. K.-A. Suominen, J. Phys. B **29**, 5981 (1996).
10. S.C. Zilio, L. Marcassa, S. Muniz, R. Horowicz, V. Bagnato, R. Napolitano, J. Weiner, P.S. Juliennne, Phys. Rev. Lett. **76**, 2033 (1996).
11. H.C. Mastwijk, Ph.D. thesis, Utrecht, 1997.
12. M.W. Müller, A. Merz, M.-W. Ruf, H. Hotop, W. Meyer, M. Movre, Z. Phys. D **21**, 89 (1991).
13. W. Allison, E.E. Muschlitz, J. Elec. Spectr. **23**, 339 (1981).
14. F. Bardou, O. Emile, J.-M. Courty, C.I. Westbrook, A. Aspect, Europhys. Lett. **20**, 681 (1992).
15. H.C. Mastwijk, J.W. Thomsen, P. van der Straten, A. Niehaus, Phys. Rev. Lett. (submitted, 1998).
16. A. Gallagher, D.E. Pritchard, Phys. Rev. Lett. **63**, 957 (1989)
17. M.J. Holland, K.-A. Suominen, K. Burnett, Phys. Rev. A **50**, 1513 (1994).
18. P.S. Julienne, J. Vigué, Phys. Rev. A **44**, 4464 (1991).